

## Rab4A GTPase–Catenin Interactions Are Involved in Cell Junction Dynamics in the Testis

DOLORES D. MRUK,\* ANN S. N. LAU,\* OLI SARKAR,\* AND WEILIANG XIA\*

From the \*Population Council, Center for Biomedical Research, New York, New York.

**ABSTRACT:** A plethora of evidence has recently accumulated to suggest that Rab guanosine triphosphates (GTPases) may have functions other than those originally proposed in vesicle formation, movement, docking, and fusion. Studies have shown, for example, that Rab proteins interact with actin filaments and microtubules, illustrating cross-talk between intracellular transport and cytoskeletal dynamics. In this report, we show that Rab4A associates with adherens junction signaling proteins in the testis. By immunoprecipitation, Rab4A was found to interact with  $\alpha$ - and  $\beta$ -catenin as well as with actin, vimentin,  $\alpha$ - and  $\beta$ -tubulin, and protein kinase C (PKC)- $\alpha$  and  $\epsilon$ . Additionally, administration of Adjudin to adult rats up-

regulated the Rab4A level, which coincided with the loss of spermatocytes, round and elongating/elongated spermatids from the seminiferous epithelium. More importantly, the ability of Rab4A to associate with  $\alpha$ - and  $\beta$ -catenin increased during Adjudin-induced junction restructuring in the testis, illustrating that Rab4A–catenin interactions are likely to be involved in the disassembly of Sertoli–germ cell contacts. Taken collectively, these results suggest that Rab4A participates in adherens junction dynamics.

Key words: Adherens junction, Sertoli cell, germ cell.

J Androl 2007;28:742–754

The assembly of an adherens junction between 2 cells—which entails that cadherins, catenins, and other molecules assemble into a functional protein complex—is not a simple process but one that involves an array of cellular events (Braga, 2002; Cheng and Mruk, 2002; Perez-Moreno et al, 2003; Mruk and Cheng, 2004). For example, epithelial cells must use the cytoskeletal network, which is composed of actin microfilaments, intermediate filaments, and microtubules, to ensure that newly synthesized proteins are efficiently delivered to the appropriate cell surface domain prior to junction assembly (Mays et al, 1994; Bryant and Stow, 2004). Although the precise role of the cytoskeleton in protein delivery is not entirely known, studies have indicated that actin microfilaments and microtubules serve as guides or tracks for the movement of vesicles containing cargo (eg, proteins and lipids). In recent years, we have learned that Rab guanosine triphosphates (GTPases) participate in these events (Yeaman et al, 1999; Apodaca, 2001). Rab GTPases are guanosine 5'-triphosphate (GTP)-binding signaling molecules of approximately 20–30 kDa that cycle

between guanosine diphosphate (GDP)-bound, membrane (active) and GDP-bound, cytosolic (inactive) forms. Three types of regulatory proteins orchestrate this activation and inactivation: 1) GDP/GTP exchange protein (GEP), 2) GTPase activating protein (GAP), and 3) GDP dissociation inhibitor (GDI). Collectively, they allow Rab GTPases to temporally and spatially regulate diverse cellular events such as vesicle movement, transcytosis, recycling, endocytosis, exocytosis, cytoskeletal organization, and cell polarity (Somsel Rodman and Wandinger-Ness, 2000; Seabra and Coudrier, 2004). Thus, a Rab GTPase is analogous to a bus with passengers (cargo) traveling along a designated route (cytoskeletal network). During its journey, this bus will verge upon several traffic lights that will instruct it either to go (GTP-bound conformation) or stop (GDP-bound conformation), depending on regulatory cues received from other vehicles (GEP, GAP, and GDI). Upon arriving at its final destination (docking), passengers will be discharged from the bus so that they may carry out their unique roles at this specific site.

In this study, we ask whether there is a connection between Rab GTPases and adherens junction dynamics. We pose this question because the adherens junction has been shown time and time again to integrate a wide range of signals to regulate cell adhesion. For instance, the formation of focal adhesions (cell–extracellular matrix anchoring junctions in which the cytoplasmic face of cells is linked to actin) as well as cell movement were affected in Swiss 3T3 cells when the transport of vesicles to and

Supported in part by a grant from the CONRAD Program (CICCR, CIG-01-74) (D.D.M.).

Correspondence to: Dr Dolores D. Mruk, Population Council, Center for Biomedical Research, 1230 York Ave, New York, NY 10021 (e-mail: mruk@popcbr.rockefeller.edu).

Received for publication November 18, 2006; accepted for publication May 7, 2007.

DOI: 10.2164/jandrol.106.002204

from the plasma membrane was inhibited by brefeldin A, a fungal metabolite known to inhibit protein secretion (Bershadsky and Futerman, 1994). This finding points to the existence of a relationship between junction integrity, cell movement, and vesicle transport. In a recently published study, we reported that Rab8B, a GTPase that functions in the transport of vesicles to the plasma membrane, associated with the E-cadherin- $\gamma$ -catenin protein complex in Sertoli cells as determined by chemical crosslinking and immunoprecipitation experiments (Lau and Mruk, 2003). Also, the level of Rab8B was observed to increase during the assembly of adherens junctions in vitro (Lau and Mruk, 2003). While these findings provided early evidence of Rab GTPase function at the adherens junction, they were not entirely unexpected, because the participation of Rabs in tight junction dynamics had already been established in previously published reports (Sheth et al, 2000; Marzesco et al, 2002). Additionally, more recent studies have shown that Rab GTPases coordinate the internalization of E-cadherin during junction disassembly (Palacios et al, 2001; Maxfield and McGraw, 2004; Lock and Stow, 2005). In this study, we demonstrate that another Rab family member, Rab4A, has a role similar to that of Rab8B at the adherens junction. We describe herein the interaction of Rab4A with  $\alpha$ - and  $\beta$ -catenin—2 adherens junction signaling proteins that link cadherin to the cytoskeleton—in the testis. As important, the ability of Rab4A to associate with  $\alpha$ - and  $\beta$ -catenin increased when the integrity of adherens junctions between Sertoli and germ cells was compromised by Adjudin (formerly known as AF-2364 or 1-(2,4-dichlorobenzyl)-1H-indazole-3-carbohydrazide) (Cheng et al, 2001; Grima et al, 2001; Mruk and Cheng, 2004). Taken collectively, these results provide an unprecedented opportunity to expand in future studies the role of Rab GTPases in cell junction dynamics.

## Methods

### *Animals*

Sprague-Dawley rats were purchased (Charles River Laboratories, Kingston, NY) and allowed to acclimate at The Rockefeller University's Laboratory Animal Research Center for 24–48 hours before use. Animals had access to rat chow and water ad libitum and were exposed to 12-hour light—12-hour dark cycles. Rats were sacrificed by CO<sub>2</sub> asphyxiation as directed in the 2000 Report of the American Veterinary Medical Association (AVMA) Panel on Euthanasia (Beaver et al, 2001). The use of animals in this study was approved by The Rockefeller University Animal Care and Use Committee (Protocol Nos. 00111 and 03017).

### *Antibodies and Reagents*

The following antibodies were purchased from Santa Cruz Biotechnology Inc (Santa Cruz, Calif): anti-Rab4A (Catalog No. sc-312, Lot Nos. D0904 and G012), antiactin (Catalog No. sc-7210, Lot No. G1404, and Catalog No. sc-1616, Lot No. H2604), anti-vimentin (Catalog No. sc-6260, Lot No. B252, and Catalog No. sc-5565, Lot No. E012), anti- $\beta$ -tubulin (Catalog No. sc-9104, Lot No. I1602), anti- $\gamma$ -tubulin (Catalog No. sc-10732, Lot No. A311), anti-protein kinase C (PKC)- $\alpha$  (Catalog No. sc-208, Lot No. H052), anti-PKC- $\epsilon$  (Catalog No. sc-214, Lot No. G192), anti-E-cadherin (Catalog No. sc-7870, Lot Nos. K080, C212, and G1403), anti- $\alpha$ -catenin (Catalog No. sc-7894, Lot No. E141), and anti-integrin  $\beta$ 1 (Catalog No. sc-8978, Lot No. E0203). The following antibodies were purchased from Invitrogen (Carlsbad, Calif): antioccludin (Catalog No. 71-1500, Lot No. 11067632), anti-ZO-1 (Catalog No. 33-9100, Lot Nos. 20269234 and 31085202), anti-ZO-2 (Catalog No. 71-1400, Lot No. 20671338), anti-N-cadherin (Catalog No. 33-3900, Lot Nos. 20671409, 30778768, and 31185680), anti- $\beta$ -catenin (Catalog No. 71-2700, Lot Nos. 11067640 and 30477187), and anti- $\gamma$ -catenin (Catalog No. 13-8500, Lot No. 20772586). In addition, another Rab4A antibody was purchased from Calbiochem (San Diego, Calif) (Catalog No. 552104, Lot No. D20020). Secondary antibodies consisted of bovine anti-rabbit, anti-mouse, or anti-goat immunoglobulin G (IgG) conjugated to horseradish peroxidase (HRP) (Santa Cruz). Recombinant Rab4A (Catalog No. 552107, Lot No. B20435), which was used as a positive control in selected immunoblotting experiments, was obtained from Calbiochem.

### *Sertoli Cell Cultures*

Sertoli cell cultures were prepared from 20-day-old rat testes by sequential enzymatic treatments (Cheng et al, 1986; Mruk et al, 2003). Cells were plated at high density ( $0.75 \times 10^6/\text{cm}^2$ ) on Matrigel (diluted 1:7 with Ham's F-12 Nutrient Mixture and Dulbecco modified Eagle medium [F-12/DMEM], 1:1; Sigma, St Louis, Mo)-coated 6-well dishes in F-12/DMEM supplemented with growth factors as previously described (Cheng et al, 1986; Mruk et al, 2003). Sertoli cell plating density was determined by obtaining the volume of sedimented cells following brief centrifugation at  $800 \times g$ . For instance, a packed cell volume of 0.5 mL corresponded to about  $180 \times 10^6$  Sertoli cells. This ratio was obtained by plating Sertoli cells isolated from the testes of 10 rats (20 days old) on 100-mm dishes, followed by a hypotonic treatment on day 2 to yield Sertoli cells with a purity greater than 98% (Galdieri et al, 1981). Thereafter,

Sertoli cells were trypsinized on day 5, the packed cell volume obtained by centrifugation, and cells counted with a hemocytometer. This was routinely done over the course of several years to generate a table to describe the reciprocal relationship between packed Sertoli cell volume and the number of Sertoli cells isolated. Given that Sertoli cells are in small aggregates at the time of plating, this is the most fitting way that we could assess the yield of Sertoli cells isolated and the plating cell density. For Sertoli cells plated at high density, media were replaced every 24 hours, and Sertoli cells were incubated for a total of 5 days to allow the assembly of cell junctions to complete. Cells were terminated on day 6 in immunoprecipitation (IP) lysis buffer (50 mM Tris, pH 7.4, at 22°C containing 0.15 M NaCl, 1% Nonidet P-40 [vol/vol], 10% glycerol [vol/vol], 2 mM 4-(2-aminoethyl)benzenesulfonyl fluoride [AEBSF], 1 mM EDTA, 100 µM bestatin, 15 µM E-64, 1 µM aprotinin, 1 µM leupeptin, 1 mM Na<sub>3</sub>VO<sub>4</sub>, and 1 mM NaF).

#### *Isolation of Germ Cells*

Germ cells were isolated from 90-day-old rat testes as previously described (Aravindan et al, 1996, 1997). In this study, germ cell preparations were not exposed to glass wool filtration and thus consisted of spermatogonia, spermatocytes, round and elongating/elongated spermatids, and spermatozoa. Germ cell purity was assessed by reverse transcription–polymerase chain reaction (RT-PCR) and/or immunoblotting as previously described (Chung and Cheng, 2001; Lee et al, 2004) using putative Sertoli (eg, occludin, testin) (Grima et al, 1995; Moroi et al, 1998), Leydig (eg, 3β-hydroxysteroid dehydrogenase) (Baillie and Griffiths, 1964), and peritubular myoid (eg, alkaline phosphatase and fibronectin) (Palombi and Di Carlo, 1988) cell products. Following isolation, germ cells were terminated immediately in IP lysis buffer or RNA STAT 60 (Tel Test “B,” Friendswood, Tex).

#### *Semiquantitative RT-PCR*

Semiquantitative RT-PCR was performed as previously described (Mruk and Cheng, 1999; Lau and Mruk, 2003). Primers used for the amplification of Rab4A (Zahraoui et al, 1988) and S16 (Chan et al, 1990) were as follows: 5′–GGAAATGCGGGAAGTGGCAAATC–3′ (Rab4A sense, nucleotides 43–65), 5′–CCTGTGCAC TTGGAGCCTGTGTAC–3′ (Rab4A anti-sense, nucleotides 605–628), 5′–TCCGCTGCAGTCCGTTCAA GTCTT–3′ (S16 sense, nucleotides 15–38), and 5′–GCCAACTTCTTGGATTTCGACG–3′ (S16 anti-sense, nucleotides 376–399). To obtain semiquantitative data, Rab4A and S16 sense primers (approximately 0.2 µg each) were 5′-end-labeled with [ $\gamma$ -<sup>32</sup>P] adenosine 5′-

triphosphate (ATP [specific activity, 6000 Ci/mmol; Amersham Biosciences Corp, Piscataway, NJ]) by using T4 polynucleotide kinase (Promega, Madison, WI). Thereafter, labeled primers were incorporated into PCR reaction tubes, a total of 23 cycles run, and PCR products visualized by autoradiography. To ensure that the amplifications of both Rab4A and S16 were in the linear range of cDNA production, a series of preliminary studies was performed in which different concentrations of Rab4A and S16 primers were combined with testis cDNA templates for cycling at different annealing temperatures (Mruk et al, 1998; Mruk and Cheng, 1999).

#### *Cell and Tissue Lysates, Immunoprecipitation, SDS-PAGE, and Immunoblotting*

Cell and tissue lysates were obtained by sonicating samples on ice, centrifuging suspensions at 15 000 × g, and collecting supernatants. For immunoprecipitation, protein lysates (eg, 300 µg Sertoli cell lysate; 500 µg each seminiferous tubule and testis lysates) were pretreated with normal serum on a rotator, followed by the addition of Protein A/G PLUS agarose (Santa Cruz). Thereafter, supernatants were incubated with different antibodies (about 2 µg IgG per sample) as specified. Immunocomplexes, precipitated by adding Protein A/G PLUS agarose, were washed extensively with immunoprecipitation wash buffer (50 mM Tris, pH 7.4, at 22°C containing 0.15 M NaCl, 1% Nonidet P-40 [vol/vol], protease and phosphatase inhibitors). Proteins were extracted from agarose beads by heating in SDS-sample buffer (0.125 M Tris, pH 6.8, at 22°C containing 1% SDS [wt/vol], 20% glycerol [vol/vol], and 1.6% β-mercaptoethanol [vol/vol]) and samples electrophoresed by sodium dodecyl sulfate–polyacrylamide gel electrophoresis (SDS-PAGE). Following electrophoresis, proteins were electroblotted onto a nitrocellulose membrane (Schleicher & Schuell, Keene, NH), nonspecific sites blocked with blocking buffer (6% nonfat milk [wt/vol] in phosphate-buffered saline [PBS]–Tris buffer [10 mM sodium phosphate, pH 7.4, at 22°C containing 0.15 M NaCl, 10 mM Tris, and 0.1% Tween-20 (vol/vol)], and the blot incubated in primary antibody. Thereafter, the blot was briefly washed with PBS-Tris buffer and incubated in secondary antibody. Immunoreactive bands were detected by enhanced chemiluminescence. The Rab4A antibody that was used for immunoprecipitation was obtained from Calbiochem (Catalog No. 552104, Lot No. D20020). For routine immunoblotting experiments that did not employ immunoprecipitation, approximately 75–100 µg of protein from cell or tissue lysates was electrophoresed by SDS-PAGE under reducing conditions and proteins electroblotted onto a nitrocellulose membrane for immunoblotting as described.

### Immunohistochemistry

Adult rats (250–300 g body weight) were killed, testes removed, and immediately fixed in Bouin's Fixative. Tissues were processed routinely, embedded in paraffin wax, and blocks cut to generate 5- $\mu$ m sections. Immunostaining was performed by using a Histostain-SP kit (Invitrogen) as instructed by the manufacturer with minor modifications. Sections were deparaffinized in xylene, rehydrated in descending concentrations of ethanol, and washed with PBS (10 mM sodium phosphate, pH 7.4, at 22°C containing 0.15 M NaCl). Endogenous peroxidase activity was blocked with 3% hydrogen peroxide (vol/vol). Thereafter, sections were permeabilized (0.2% Triton X-100 [vol/vol]) and non-specific sites blocked overnight with 10% nonimmune goat serum (vol/vol), followed by incubation with anti-Rab4A antibody (1:100 dilution) at room temperature overnight. Sections were then saturated with biotinylated goat anti-rabbit secondary antibody, followed by streptavidin-HRP. Immunoreactive Rab4A was visualized by 3-amino-9-ethyl carbazole (AEC). Sections were counterstained with hematoxylin and mounted for microscopy. Images were captured and compiled using Photoshop Software (version 7.0, Adobe Systems Inc, San Jose, Calif). Controls included incubating sections with PBS, nonimmune rabbit IgG (1:100 dilution), or an anti-Rab4A antibody preabsorbed with recombinant Rab4A in place of primary antibody. Immunostaining was also repeated using frozen sections as previously described (Lau and Mruk, 2003). In another series of experiments, immunostaining was performed using paraffin-embedded testes obtained from rats at 12 (blood-testis barrier [BTB] not yet formed), 15 (BTB beginning to form), and 25 days of age (BTB already formed) (Vitale et al, 1973; Gilula et al, 1976; Russell et al, 1989).

### Immunofluorescence

Immunofluorescence was performed using Sertoli cells cultured on thermanox plastic coverslips (Nunc, Rochester, NY) at low ( $5 \times 10^4/\text{cm}^2$ ) and high ( $0.25 \times 10^6/\text{cm}^2$ ) densities. Cells were terminated on day 5 and fixed in 3.7% paraformaldehyde (wt/vol). Fixative was removed by successive washes in PBS, and cells were permeabilized and saturated in 10% nonimmune goat serum (vol/vol) for 90–120 minutes. Thereafter, Sertoli cells were incubated in anti-Rab4A antibody (1:300 dilution) containing 1% bovine serum albumin (BSA) (wt/vol) at room temperature overnight. The following day, cells were washed and incubated in goat anti-rabbit IgG-fluorescein isothiocyanate (FITC [1:100 dilution; Invitrogen]) containing 1% nonimmune goat serum (vol/vol). After washing, cells were mounted using antifade reagent (50% glycerol [vol/vol] in PBS, pH 7.4, at 22°C

containing 0.1%  $\text{NaN}_3$  [wt/vol]) for microscopy. Controls included incubating cells with PBS or nonimmune rabbit IgG (1:300 dilution) in place of primary antibody.

### Treatment of Rats with Adjuvin

A single dose (50 mg/kg body weight) of Adjuvin suspended in 0.25% methylcellulose (wt/vol) was administered to adult rats (250–300 g body weight,  $n = 5$ –7 rats per time point) by gavage as previously described (Cheng et al, 2001; Grima et al, 2001). Control animals received only methylcellulose. Thereafter, rats were killed at specified time points and testes removed for the preparation of tissue lysates or paraffin processing.

### General Methods

To assess the suitability of the anti-Rab4A antibody for immunohistochemistry, a series of preliminary experiments was performed by immunoblotting using 6 different antibodies. In brief, 100  $\mu$ g testis lysate was combined with reducing (0.125 M Tris, pH 6.8, at 22°C containing 1% SDS [wt/vol], 20% glycerol [vol/vol], and 1.6%  $\beta$ -mercaptoethanol [vol/vol]) or nonreducing (0.125 M Tris, pH 6.8, at 22°C containing 1% SDS [wt/vol] and 20% glycerol [vol/vol]) SDS-sample buffer, heated at 100°C, and electrophoresed by SDS-PAGE. In another set of testis lysates, samples were processed identically except that heating was omitted prior to electrophoresis. The antibody that cross-reacted strongly with Rab4A but minimally with other testicular proteins was used for immunohistochemistry (Santa Cruz; Catalog No. sc-312, Lot Nos. D0904 or G012). The preabsorbed Rab4A antibody was obtained by incubating the selected anti-Rab4A antibody (1:100 dilution) with recombinant Rab4A (0.5  $\mu$ g). Thereafter, antibody-antigen immunocomplexes were precipitated by adding anti-rabbit IgG (whole molecule)–agarose (Sigma) and the supernatant used for immunohistochemistry. Nonimmune rabbit IgG was prepared by ammonium sulfate precipitation and diethylaminoethyl (DEAE)-chromatography as previously described (Cheng et al, 1988; Page and Thorpe, 2001a,b). Seminiferous tubules were isolated from 90-day-old rat testes and cultured as described (Zwain and Cheng, 1994; Lee et al, 2003). Thereafter, tubule cultures were terminated in IP lysis buffer for the preparation of lysates. In another experiment, staged seminiferous tubules were isolated by transillumination-assisted dissection (Parvinen and Vanha-Perttula, 1972; Parvinen and Ruokonen, 1982; Chen et al, 2003). The wave of the seminiferous cycle was dissected into 4 distinct zones: pale (stages IX–XII), weak spot (stages XIII–I), dark spot (stages II–VI), and long dark (stages VII–VIII). Tubules were resuspended in IP lysis buffer or

RNA STAT 60. Prior to using staged tubules for Rab4A analysis, RT-PCR was performed using cathepsin L primers as previously described (Chung et al, 1998; Chen et al, 2003). Because cathepsin L is stage-specific in the testis (Wright et al, 1995), it was used as a marker to assess the staging of seminiferous tubules. In selected experiments, immunoblots were stripped with stripping buffer (62.5 mM Tris, pH 6.7, at 22°C containing 100 mM  $\beta$ -mercaptoethanol and 2% SDS [wt/vol]) and reprobed with another primary antibody. Protein concentration was determined by Coomassie blue dye-binding assay using BSA as a standard (Bradford, 1976). The authenticity of the Rab4A PCR product was verified by nucleotide sequencing using Sequenase (Cheng et al, 1988). Statistical analyses were performed by either Student's *t* test or analysis of variance using InStat Software (version 3.01; Graph Pad Software Inc, San Francisco, Calif). Densitometric scanning was performed using QuantiScan Software (version 3.0; Biosoft, Ferguson, Mo). All experiments reported in this paper were repeated 3–5 times.

## Results

### *Rab4A Is Produced by Sertoli and Germ Cells*

By RT-PCR (Figure 1A and B) and immunoblotting (Figure 1C) Rab4A was found to be present in the rat testis. During testicular development, the Rab4A mRNA level increased approximately 10-fold from 10–20 days of age, and it remained at this elevated level until 90 days of age (Figure 1A and B). The 586-bp PCR product (Figure 1A) was sequenced and confirmed to be Rab4A. At the cellular level, immunoreactive Rab4A (22 kDa) was detected by immunoblotting in Sertoli as well as in germ cells isolated from 20- and 60-day-old testes, respectively (Figure 1C). By immunofluorescence, Rab4A's localization in low density Sertoli cell cultures ( $0.05 \times 10^6/\text{cm}^2$ ) was restricted to the cytoplasm (Figure 1D, arrows). Immunoreactivity corresponding to Rab4A was also consistently detected in the nucleus (Figure 1D, arrowheads). When high density Sertoli cell cultures ( $0.25 \times 10^6/\text{cm}^2$ ) were used for immunofluorescence experiments, Rab4A immunoreactivity was likewise restricted to the cytoplasm (Figure 1E). Replacing the primary antibody with PBS (data not shown) or nonimmune rabbit IgG (Figure 1F) yielded no detectable staining.

### *Localization of Rab4A to Sertoli and Germ Cells and to Cells Within the Intertubular Region of the Testis*

Immunoreactive Rab4A was detected in all stages of the seminiferous epithelial cycle (Figure 2A through G and J). Within the seminiferous epithelium, Rab4A localized

predominantly to the Sertoli cell stalk (Figure 2A, arrows). Notably, Rab4A was found to encircle the periphery of seminiferous tubules in the basal compartment (Figure 2A and B, arrowheads). Immunoreactive Rab4A was also found in the adluminal compartment surrounding elongated spermatids (Figure 2B, arrows). Rab4A immunoreactivity was significantly weaker in spermatogonia and primary and some secondary spermatocytes, but Leydig cells were strongly reactive for this Rab GTPase (Figure 2A, white asterisks). Replacing the primary antibody with PBS (data not shown), nonimmune rabbit IgG (data not shown), or an anti-Rab4A antibody preabsorbed with recombinant Rab4A (Figure 2H) yielded no detectable staining. Overall, the intensity of Rab4A immunostaining in the adult testis was weaker when frozen sections were used, possibly due to a semicompromised morphology, but results were similar to those shown in Figure 2A through G. The immunoblot shown in Figure 2I demonstrates that the anti-Rab4A antibody (Santa Cruz; Catalog No. sc-312, Lot No. D0904) used for immunohistochemistry cross-reacted specifically with Rab4A. Figure 2J illustrates that the Rab4A level did not change significantly during different stages of the epithelial cycle. This observation is consistent with the immunohistochemistry results shown in Figure 2A through G.

On the other hand, Rab4A immunoreactivity was barely detectable within the seminiferous epithelium when paraffin sections from 12- and 15-day-old testes were used for immunohistochemistry (Figure 2K and L), although weak immunoreactivity was seen to associate with Leydig cells (Figure 2K and L, arrowheads). This observation is consistent with RT-PCR results shown in Figure 1A and B. Following the formation of the BTB at 25 days of age, an increase in Rab4A immunoreactivity was seen associating strongly with Leydig cells (Figure 2M, white asterisks) as well as with Sertoli cells (Figure 2M, arrowheads).

### *Rab4A Coimmunoprecipitates With Cell Junction Proteins*

To determine whether Rab4A associates with adherens and tight junction proteins, a series of immunoprecipitation experiments was performed. When Sertoli cell, seminiferous tubule, and testis lysates were used for immunoprecipitation in conjunction with different antibodies, Rab4A was found to interact with actin, vimentin,  $\alpha$ - (weakly) and  $\beta$ -tubulin, and  $\alpha$ - and  $\beta$ -catenin but not with  $\gamma$ -tubulin, occludin, ZO-1, ZO-2, E- and N-cadherin,  $\gamma$ -catenin, and integrin  $\beta$ 1 (Figure 3). Rab4A was also found to associate with PKC- $\alpha$  and - $\epsilon$  (weakly) (Figure 3). As a control, anti-Rab4A antibody was used for immunoprecipitation, followed by immu-

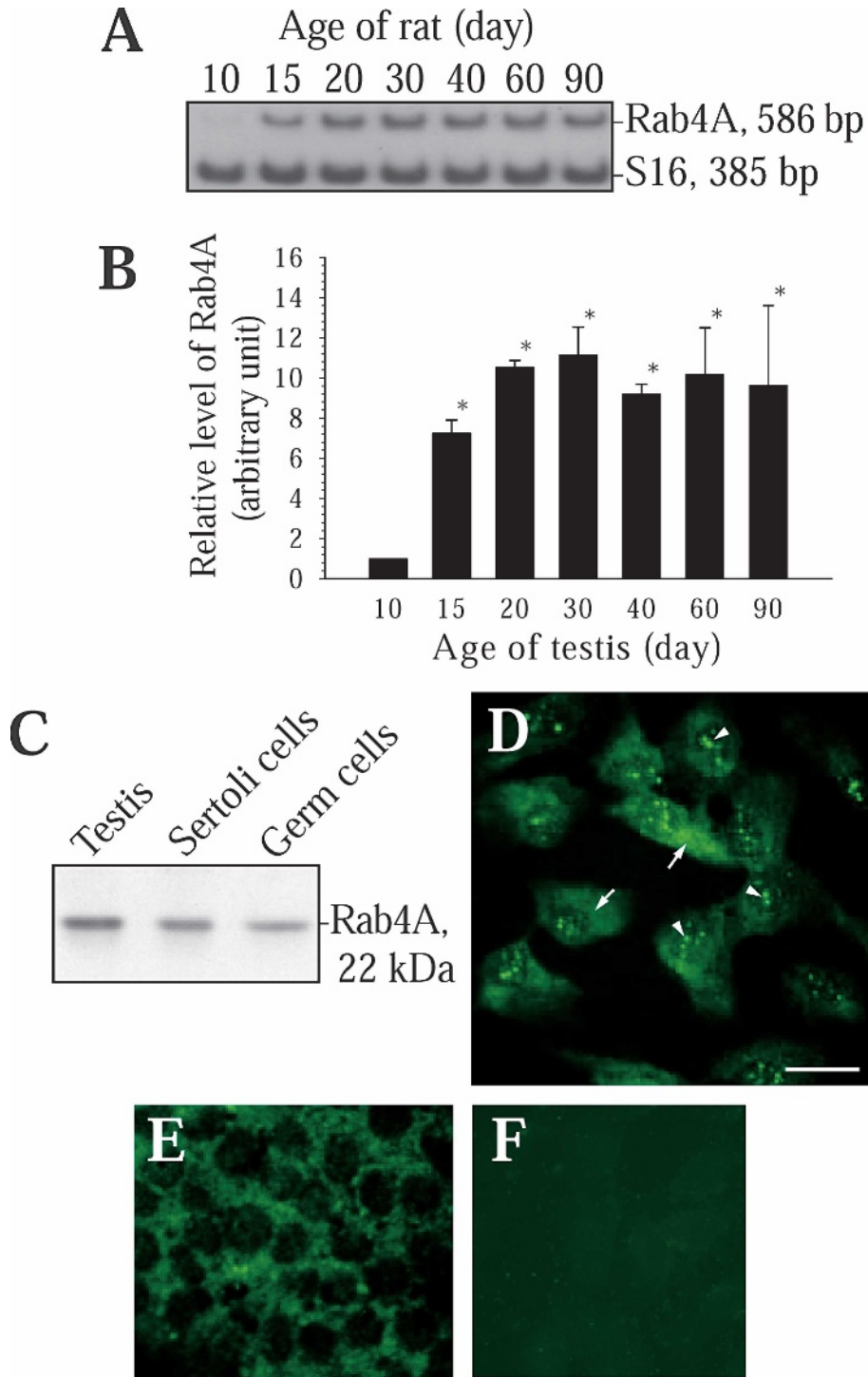


Figure 1. Partial characterization of Rab4A in the rat testis. Examination of Rab4A in the testis during development. **(A)** Autoradiogram from a reverse transcription–polymerase chain reaction (RT-PCR) experiment showing an increase in Rab4A during testicular maturation. Coamplification was performed with S16. **(B)** Densitometric scanning results from at least 3 independent RT-PCR experiments. Each Rab4A data point was first normalized against its corresponding S16 data point, followed by a second round of normalizations against testis at 10 days of age. The control was arbitrarily set at 1. \*Significantly different from testis at 10 days of age by Student's *t* test, *P* < .01. Comparative analysis of the Rab4A level in testis and Sertoli and germ cells. **(C)** Autoradiogram corresponding to an immunoblot showing Rab4A as an immunoreactive band of 22 kDa in testis and Sertoli and germ cells. Immunolocalization of Rab4A in Sertoli cells. **(D)** Micrograph of Sertoli cells cultured at low density ( $5 \times 10^4/\text{cm}^2$ ) showing that Rab4A localized to the cytoplasm (arrows) and nucleus (arrowheads). **(E)** Micrograph of Sertoli cells cultured at high density ( $0.25 \times 10^6/\text{cm}^2$ ) illustrating that Rab4A localized to the cytoplasm. **(F)** Negative control: Sertoli cells incubated with rabbit IgG instead of primary antibody. Bar = 10  $\mu\text{m}$ .

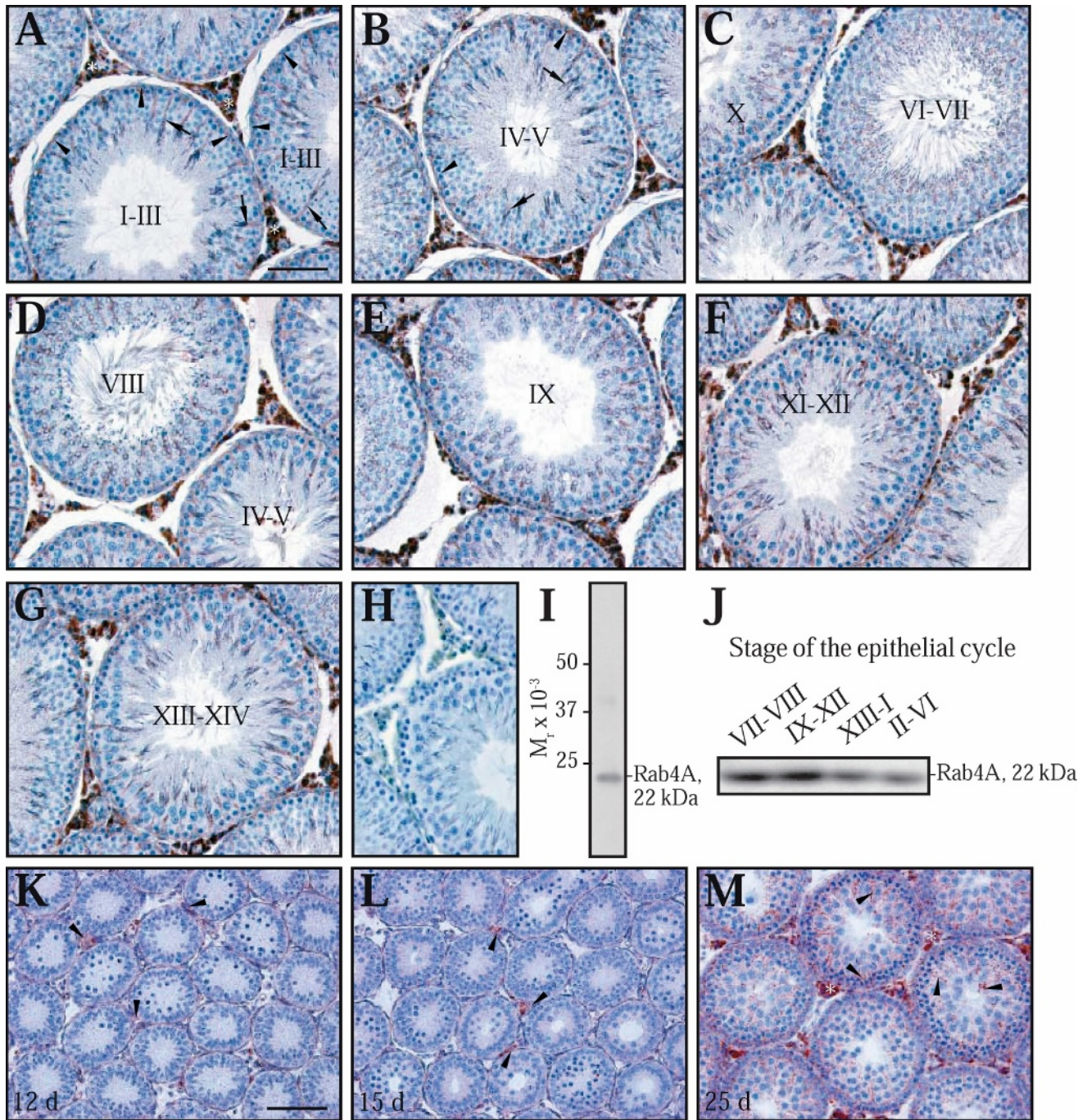


Figure 2. Immunodetection of Rab4A during the seminiferous epithelial cycle in the rat testis. Immunolocalization of Rab4A in the adult testis. **(A-H)** Cross-sections of seminiferous tubules spanning different stages of the epithelial cycle. Immunoreactive Rab4A was detected as reddish brown precipitates in Sertoli and, to a lesser extent, in germ cells in all stages of the epithelial cycle. Specifically, Rab4A localized to the basal (arrowheads, **A, B**) and adluminal (arrows, **A, B**) compartments. Immunoreactive Rab4A was also found in Leydig cells (white asterisks, **A**). Stages of the epithelial cycle are noted in roman numerals. **(H)** Cross-section of seminiferous tubules incubated with an anti-Rab4A antibody preabsorbed with recombinant Rab4A (control) and used for immunohistochemistry at the same conditions reported for **A-G**, illustrating no immunoreactivity. Bar = 75  $\mu$ m. Analysis of Rab4A antibody used for immunohistochemistry. **(I)** Autoradiogram corresponding to an immunoblot showing Rab4A as a single immunoreactive band of 22 kDa in testis. Detection of Rab4A in staged seminiferous tubules. **(J)** Autoradiogram corresponding to an immunoblot showing no significant changes in the Rab4A level in staged tubules, consistent with immunohistochemistry results (**A-G**). Immunolocalization of Rab4A in the developing testis. **(K-M)** Cross-sections of seminiferous tubules from 12- (**K**), 15- (**L**), and 25- (**M**) day-old testes. Weak Rab4A immunoreactivity was seen to associate with Leydig cells in 12- and 15-day-old testes (arrowheads, **K and L**), whereas in the 25-day-old testis Rab4A localized to Leydig cells (white asterisks, **M**) as well as to Sertoli cells (arrowheads, **M**).

		Immunoprecipitation: anti-Rab4A antibody				
Immunoblotting:		Ctrl	SCL	STL	TL	Antibody Vendor, Catalog and Lot No.
Cytoskeletal proteins	Actin					Boehringer Mannheim 1378996, Clone C4
	Vimentin					Santa Cruz sc-6260, Lot # B252
	$\alpha$ -Tubulin					Santa Cruz sc-5546, Lot # D042
	$\beta$ -Tubulin					Santa Cruz sc-9104, Lot # I1602
	$\gamma$ -Tubulin					Santa Cruz sc-10732, Lot # A311
Tight junction- and tight junction- associated proteins	Occludin					Zymed 71-1500, Lot # 11067632
	ZO-1					Zymed 33-9100, Lot # 20269234
	ZO-2					Zymed 71-1400, Lot # 20671338
	PKC- $\alpha$					Santa Cruz sc-208, Lot # H052
	PKC- $\epsilon$					Santa Cruz sc-214, Lot # G192
Adherens junction- proteins	E-Cadherin					Santa Cruz sc-7870, Lot # K080
	N-Cadherin					Zymed 33-3900, Lot # 20671409
	$\alpha$ -Catenin					Santa Cruz sc-7894, Lot # E141
	$\beta$ -Catenin					Zymed 71-2700, Lot # 11067640
	$\gamma$ -Catenin					Zymed 13-8500, Lot # 20772586
Control	Integrin $\beta$ 1					Santa Cruz sc-8978, Lot # E0203
	Rab4A					Calbiochem 552104, Lot # D20020

Figure 3. Interaction of Rab4A with cell junction proteins in the rat testis. Coimmunoprecipitation was performed using Sertoli cell (SCL), seminiferous tubule (STL), and testis (TL) lysates and an anti-Rab4A antibody. Immunoblotting was performed using antibodies as listed in the left column. Autoradiograms corresponding to different immunoblots showing Rab4A interacted with cytoskeleton (actin, vimentin,  $\alpha$ -tubulin, and  $\beta$ -tubulin), tight (PKC- $\alpha$  and PKC- $\epsilon$ ) and adherens junction- ( $\alpha$ -catenin and  $\beta$ -catenin) associated proteins. As a control, immunoprecipitation was carried out with an anti-Rab4A antibody, followed by immunoblotting with the same antibody. The first column represents Sertoli cell lysate (without immunoprecipitation) electrophoresed simultaneously with immunoprecipitation samples on the same gel and probed with the corresponding antibody as listed in the left column. Information on antibody vendors, together with catalog and lot numbers, is provided in the right column. Ctrl indicates Sertoli cells isolated from testes at 20 days of age and cultured at high density ( $0.75 \times 10^6/\text{cm}^2$ ) for 5 days without immunoprecipitation.

noblotting with the same antibody. This simply demonstrated that the Rab4A antibody used in this study was suitable for subsequent immunoprecipitation experiments. Also, each immunoblot contained an additional control—that is, Sertoli cell lysate (without immunoprecipitation) electrophoresed under reducing conditions and probed with the corresponding antibody as listed to the left of the control (Ctrl) column of Figure 3. Notably, the results shown in Figure 3 are not quantitative because antibody titers, the concentrations of different antibodies, and the amounts of protein lysates used for immunoprecipitation were not constant.

#### *Rab4A and Adjudin-Mediated Restructuring of the Seminiferous Epithelium*

The level of Rab4A in the testis was investigated following administration of Adjudin. Adjudin is a chem-

ical entity that shares structural similarities with lonidamine (1-(2,4)-dichlorobenzyl-1H-indazole-carboxylic acid), which is known to severely damage stress fibers (eg, actin filaments) in Sertoli cells (De Martino et al, 1981; Silvestrini et al, 1984). The primary manifestation resulting from Adjudin treatment is the depletion of virtually all germ cell types except spermatogonia and primary spermatocytes, which reside outside of the BTB (Cheng et al, 2001; Grima et al, 2001). If 1) the contribution made by germ cells to the overall Rab4A level in the control testis (Figure 1C) and 2) the loss of germ cells following Adjudin administration are collectively taken into account, the level of Rab4A increased significantly during Adjudin-induced cell junction restructuring (Figure 4A and B). Because Rab4A immunoreactivity in the seminiferous epithelium is largely restricted to Sertoli cells, which have an elaborate

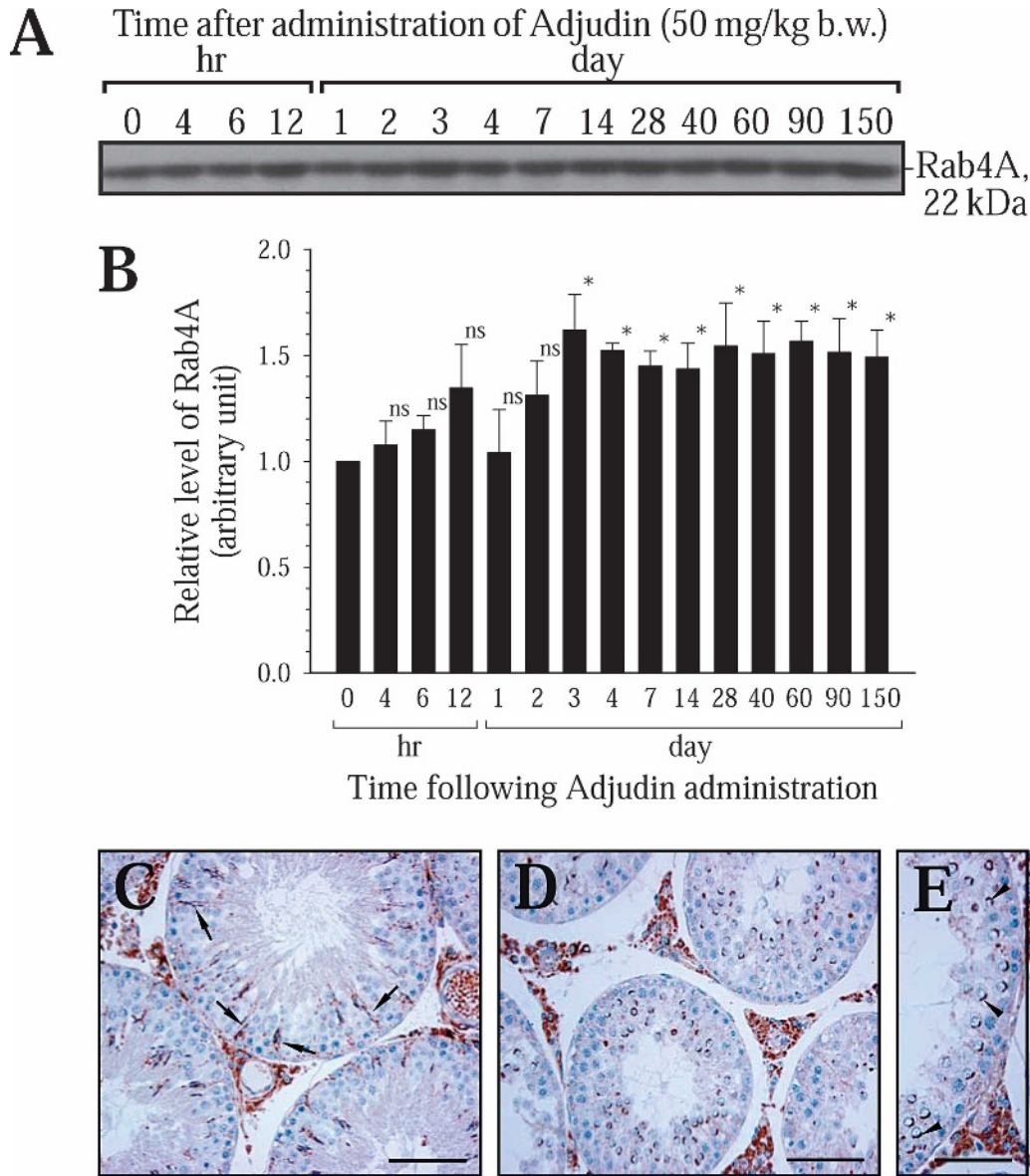


Figure 4. Participation of Rab4A in cell junction disassembly in vivo. Changes in Rab4A during Adjudin-mediated depletion of germ cells from the seminiferous epithelium. **(A)** Autoradiogram corresponding to an immunoblot showing an increase in Rab4A during germ cell loss from the epithelium. The contribution made by germ cells to the overall Rab4A level in the control testis (Figure 1C) and the loss of germ cells following Adjudin administration were both taken into account when interpreting this data. **(B)** Densitometric scanning results from at least 5 independent experiments. Each Rab4A data point was normalized against its corresponding actin data point (after stripping and reprobing the Rab4A immunoblot with an anti-actin antibody, immunoblot data not shown), followed by a second round of normalizations against testis at 0 hours (control). The control was arbitrarily set at 1. \*Significantly different from testis at 0 hours by Student's *t* test, *P* < .05; ns, not significantly different from testis at 0 hours. Immunolocalization of Rab4A in the seminiferous epithelium during Adjudin-mediated depletion of germ cells from the seminiferous epithelium. Cross-sections of seminiferous tubules 0 **(C)**, 7 **(D)**, and 14 **(E)** days after treatment. The localization of immunoreactive Rab4A (arrows) in the control testis **(C)** was similar to that shown in Figure 2A-G. By 7 **(D)** and 14 days after treatment, immunoreactive Rab4A was found to localize largely to the acrosome (arrows) of remaining germ cells. Bars in **C** and **D**, 80 μm; bar in **E**, 50 μm.

cytoskeleton (Russell, 1993), and Adjudin is proposed to target stress fibers, we have continued along this line of investigation and probed for changes in the localization of Rab4A using cross-sections from Adjudin-treated rat testes. The localization of immunoreactive Rab4A in the

control testis (Figure 4C, arrows) was consistent with results shown in Figure 2A through G. However, 7 days after Adjudin treatment, when cell junctions between remaining secondary spermatocytes and Sertoli cells were breaking down, Rab4A immunoreactivity did not

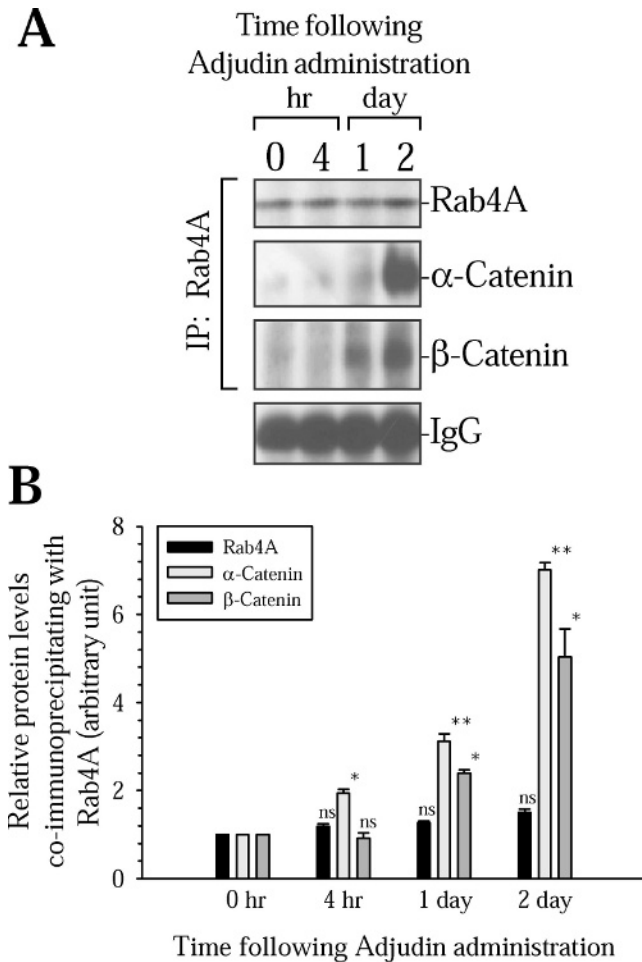


Figure 5. Adjudin-mediated junction restructuring leads to changes in Rab4A-catenin interactions in the testis. **(A)** Autoradiograms corresponding to different immunoblots showing an increase in Rab4A- $\alpha$ -catenin and Rab4A- $\beta$ -catenin coimmunoprecipitation following Adjudin administration. Immunoprecipitation was performed with anti-Rab4A antibody, whereas immunoblotting was performed using antibodies listed to the right of each immunoblot. As a control, anti-Rab4A antibody was used for immunoprecipitation, followed by immunoblotting with the same antibody (**A**, top panel), and these results were similar to those shown in Figure 4A. IgG served as an indicator of equal protein processing and loading onto gels (**A**, bottom panel). **(B)** Densitometric scanning results from at least 3 independent experiments. Each  $\alpha$ - $\beta$ -catenin data point was first normalized against its corresponding Rab4A data point, followed by a second round of normalizations against testis at 0 hours (control). The control was arbitrarily set at 1. \*Significantly different from testis at 0 hours by analysis of variance,  $P < .05$ ; \*\*Significantly different from testis at 0 hours,  $P < .01$ ; ns, not significantly different from testis at 0 hours; IP, immunoprecipitation.

localize to the Sertoli cell stalk but to the acrosome of remaining germ cells (Figure 4D versus C). Similar results were seen 14 days after treatment (Figure 4E versus C, arrowheads). Leydig cells remained strongly immunoreactive for Rab4A following Adjudin administration (Figure 4D and E versus C).

### Changes in Rab4A-Catenin Interactions During Adjudin-Mediated Junction Restructuring in the Seminiferous Epithelium

In this experiment, we assessed changes in protein-protein interactions following administration of Adjudin to adult rats. When testes lysates obtained from these animals were used for immunoprecipitation with anti- $\alpha$ - and  $\beta$ -catenin antibodies, there was a statistically significant increase in the amount of  $\alpha$ - and  $\beta$ -catenin coimmunoprecipitating with Rab4A, from 4 hours to 2 days and from 1 to 2 days, respectively (Figure 5A and B). Although Rab4A did not coimmunoprecipitate with cadherin when lysates from control testes were used (Figure 3), we proceeded nevertheless to examine whether Rab4A establishes an association with this cell adhesion protein during junction restructuring. Following Adjudin administration, however, no association was found to exist between Rab4A-E-cadherin or Rab4A-N-cadherin (data not shown). As a control, immunoprecipitation and immunoblotting were performed with an anti-Rab4A antibody using testes lysates following Adjudin treatment (Figures 5A, top panel). IgG served as an indicator of equal protein processing and loading onto gels (Figure 5A, bottom panel).

### Discussion

Rab GTPases were originally classified as regulators of traffic between distinct subcellular compartments (Somseel Rodman and Wandinger-Ness, 2000; Stenmark and Olkkonen, 2001; Takai et al, 2001; Zerial and McBride, 2001; Seachrist and Ferguson, 2003). Today, however, we know that they also function in other cellular processes. For instance, numerous studies have reported Rab-mediated endocytosis of E-cadherin during cell junction disassembly in vitro (Maxfield and McGraw, 2004; Lock and Stow, 2005; Palacios et al, 2005), a finding that has provided a new avenue in which the regulation of cell junctions can be investigated. While keeping these observations in mind, we ask in this study whether Rab4A plays a role in cell junction dynamics, because this GTPase has been shown to be a marker of the early endosome, a cellular organelle that lies in proximity to the plasma membrane. Specifically, the function of Rab4A is to coordinate protein transport from the early endosome either to the recycling endosome or to the plasma membrane (Takai et al, 2001). In the testis, Rab4A was found to be present in Sertoli and germ cells as revealed by immunoblotting and immunohistochemistry experiments. Likewise, Leydig cells were strongly immunoreactive for Rab4A,

suggesting that these cells also possess sophisticated pathways to traffic proteins between different intracellular compartments. By immunohistochemistry, discrete Rab4A staining localized to the Sertoli cell stalk in all stages of the epithelial cycle. In Sertoli cells cultured at low density *in vitro*, Rab4A was found to associate with what appeared to be cytoplasmic vesicles surrounding the perinuclear region, an observation that has been corroborated by other investigators when BHK-21 (Vitale et al, 1998; Korobko et al, 2005) and CHO (Nagelkerken et al, 2000) cells were used for immunofluorescence. Discrete Rab4A immunoreactivity was also detected in the nuclei of monolayer cultures of Sertoli (this study), BHK-21 (Vitale et al, 1998), and CHO cells (Nagelkerken et al, 2000), but the significance of this observation is not yet known. Nonetheless, Rab4A immunostaining was less apparent in germ cells, possibly because these cells have less available cytoplasm, thus making the detection of Rab4A immunoreactivity by light microscopy much more difficult. Additionally, the use of staged seminiferous tubules for immunoblotting experiments revealed that Rab4A function was equally important in all stages of the epithelial cycle. As important, testicular Rab4A surged approximately 10-fold from 10–20 days of age, after which time it remained at this elevated level. Leydig cells are apparently responsible for this increase in Rab4A, at least in part, because Rab4A immunoreactivity increased drastically in these cells during testicular development. This surge in testicular Rab4A from 10–20 days of age may also be related to the onset of a specific cellular event (eg, formation of the BTB or germ cell meiosis) and/or the cessation of a specific cellular event (eg, Sertoli cell proliferation). All of these cellular processes would require that an elaborate system be in place so that different proteins can be shuffled between distinct intracellular compartments.

Even though our understanding of endocytosis continues to grow at an exceedingly rapid rate, little is currently known about how this process and its regulatory molecules connect functionally with the cytoskeleton. For example, several cytoskeleton-associated proteins such as actin, tubulin, kinesin, and dynein (Pol et al, 1997; Qualmann et al, 2000) have been linked to the endosomal system as well as to Rab GTPase function, but the mechanisms controlling these interactions are largely unknown. In this study, we report that Rab4A physically associated with actin filaments and microtubules. This has been supported in part by Bielli and colleagues (2001), who demonstrated that Rab4A localizes to microtubules in HeLa cells. Whether Rab4A connects to the actin cytoskeleton directly or via scaffolding proteins (eg,  $\alpha$ -actinin, gelsolin, vinculin,

and espin) has not yet been completely addressed by any single study. However, we report herein the existence of a direct as well as an indirect interaction between Rab4A and actin via  $\alpha$ - and  $\beta$ -catenin, respectively. When these results are interpreted in the context of Rab4A function, they ultimately suggest that protein-protein interactions that underlie adherens junction function are not static, an observation that has been supported time and time again by different *in vitro* and *in vivo* systems (Mruk and Cheng, 2004; Erez et al, 2005; Palacios et al, 2005).

When a single dose of Adjudin was administered *in vivo* as a means to induce extensive Sertoli-germ cell junction disassembly, the level of Rab4A remained fairly constant at first examination. However, immunoblotting results have shown that the level of Rab4A in germ cells is comparable to that in Sertoli cells. Thus, Adjudin-mediated loss of germ cells from the seminiferous epithelium should in fact result in a significant decrease in the testicular Rab4A level. Instead, a surge in Rab4A was noted, implicating Rab4A in the events of junction restructuring. Additionally, the increase in Rab4A- $\alpha$ -catenin and Rab4A- $\beta$ -catenin coimmunoprecipitation after Adjudin treatment suggests that these adaptor proteins are possibly moving away from the adherens junction and associating with the early endosome of which Rab4A is a marker. Indeed,  $\beta$ -catenin was found to dissociate from N-cadherin following Adjudin administration (Xia and Cheng, 2005). It should also be noted that the levels of  $\alpha$ - and  $\beta$ -catenin do not decrease following Adjudin administration, even when virtually all Sertoli-germ cell adhesive contacts have been disassembled. These results seemingly suggest that during junction disassembly early endosome-associated catenin is possibly being trafficked to the recycling endosome. Because many germ cells have depleted the seminiferous epithelium 1 week after Adjudin treatment, the need for the BTB to disassemble transiently to allow for the entry of preleptotene spermatocytes into the adluminal compartment may not exist any longer. Thus, this may explain why a loss of Rab4A immunoreactivity was detected in the basal compartment of Sertoli cells following Adjudin administration. However, we do not know exactly why an immunoreactive signal corresponding to Rab4A would be found in the acrosome of remaining germ cells. Taken collectively, these results suggest that Rab4A likely participates in the restructuring of adherens junctions in the testis. As the number of studies reporting endocytosis-related cellular phenomena increases in coming years, it will be interesting to discover how Rab4A participates in cell junction dynamics in the seminiferous epithelium as well as in other epithelia.

## References

- Apodaca G. Endocytic traffic in polarized epithelial cells: role of the actin and microtubule cytoskeleton. *Traffic*. 2001;2:149–159.
- Aravindan GR, Mruk D, Lee WM, Cheng CY. Identification, isolation, and characterization of a 41-kilodalton protein from rat germ cell-conditioned medium exhibiting concentration-dependent dual biological activities. *Endocrinology*. 1997;138:3259–3268.
- Aravindan GR, Pineau C, Bardin CW, Cheng CY. Ability of trypsin in mimicking germ cell factors that affect Sertoli cell secretory function. *J Cell Physiol*. 1996;168:123–133.
- Baillie AH, Griffiths K.  $\beta$ -Hydroxysteroid dehydrogenase activity in the mouse Leydig cell. *J Endocrinol*. 1964;29:9–17.
- Beaver BV, Reed W, Leary S, McKiernan B, Bain F, Schultz R, Bennett BT, Pascoe P, Shull E, Cork LC, Francis-Floyd R, Amass KD, Johnson R, Schmidt RH, Underwood W, Thornton GW, Kohn B. 2000 Report of the AVMA Panel on Euthanasia. *JAVMA*. 2001;218:669–696.
- Bershadsky AD, Futerman AH. Disruption of the Golgi apparatus by brefeldin A blocks cell polarization and inhibits directed cell migration. *Proc Natl Acad Sci U S A*. 1994;91:5686–5689.
- Bielli A, Thornqvist PO, Hendrick AG, Finn R, Fitzgerald K, McCaffrey MW. The small GTPase Rab4A interacts with the central region of cytoplasmic dynein light intermediate chain-1. *Biochem Biophys Res Commun*. 2001;281:1141–1153.
- Bradford MM. A rapid and sensitive method for the quantitation of microgram quantities of protein utilizing the principle of protein-dye binding. *Anal Biochem*. 1976;72:248–254.
- Braga VMM. Cell-cell adhesion and signaling. *Curr Opin Cell Biol*. 2002;14:546–556.
- Bryant DM, Stow JL. The ins and outs of E-cadherin trafficking. *Trends Cell Biol*. 2004;14:427–434.
- Chan YL, Paz V, Olvera J, Wool IG. The primary structure of rat ribosomal protein S16. *FEBS Lett*. 1990;263:85–88.
- Chen YM, Lee NPY, Mruk DD, Lee WM, Cheng CY. Fer kinase/Fer T and adherens junction dynamics in the testis: an in vitro and in vivo study. *Biol Reprod*. 2003;69:656–672.
- Cheng CY, Chen CL, Feng ZM, Marshall A, Bardin CW. Rat clusterin isolated from primary Sertoli cell enriched culture medium is sulfated glycoprotein-2 (SGP-2). *Biochem Biophys Res Commun*. 1988;155:398–404.
- Cheng CY, Mather JP, Byer AL, Bardin CW. Identification of hormonally responsive proteins in primary Sertoli cell culture medium by anion-exchange high performance liquid chromatography. *Endocrinology*. 1986;118:480–488.
- Cheng CY, Mathur PP, Grima J. Structural analysis of clusterin and its subunits in ram rete testis fluid. *Biochemistry*. 1988;27:4079–4088.
- Cheng CY, Mruk DD. Cell junction dynamics in the testis: Sertoli-germ cell interactions and male contraceptive development. *Physiol Rev*. 2002;82:825–874.
- Cheng CY, Silvestrini B, Grima J, Mo MY, Zhu LJ, Johansson E, Saso L, Leone MG, Palmery M, Mruk D. Two new male contraceptives exert their effects by depleting germ cells prematurely from the testis. *Biol Reprod*. 2001;65:449–461.
- Chung NPY, Cheng CY. Is cadmium chloride-induced inter-Sertoli tight junction permeability barrier disruption a suitable in vitro model to study the events of junction disassembly during spermatogenesis in the rat testis? *Endocrinology*. 2001;142:1878–1888.
- Chung SS, Zhu LJ, Mo MY, Silvestrini B, Lee WM, Cheng CY. Evidence for cross-talk between Sertoli and germ cells using selected cathepsins as markers. *J Androl*. 1998;19:686–703.
- De Martino C, Malcorni W, Bellocchi M, Floridi A, Marcante ML. Effects of AF1312 TS and lonidamine on mammalian testis. A morphological study. *Chemotherapy*. 1981;27(suppl 2):27–42.
- Erez N, Bershadsky A, Geiger B. Signaling from adherens-type junctions. *Eur J Cell Biol*. 2005;84:235–244.
- Galdieri M, Ziparo E, Palombi F, Russo MA, Stefanini M. Pure Sertoli cell cultures: a new model for the study of somatic-germ cell interactions. *J Androl*. 1981;5:249–259.
- Gilula NB, Fawcett DW, Aoki A. The Sertoli cell occluding junctions and gap junctions in mature and developing mammalian testis. *Dev Biol*. 1976;50:142–168.
- Grima J, Silvestrini B, Cheng CY. Reversible inhibition of spermatogenesis in rats using a new male contraceptive, 1-(2,4-dichlorobenzyl)-indazole-3-carbohydrazide. *Biol Reprod*. 2001;64:1500–1508.
- Grima J, Zhu LJ, Zong SD, Catterall JF, Bardin CW, Cheng CY. Rat testis is a newly identified component of the junctional complexes in various tissues whose mRNA is predominantly expressed in the testis and ovary. *Biol Reprod*. 1995;52:340–355.
- Korobko E, Kiselev S, Olsnes S, Stenmark H, Korobko I. The Rab5 effector Rabaptin-5 and its isoform Rabaptin-5 $\delta$  differ in their ability to interact with the small GTPase Rab4. *FEBS J*. 2005;272:37–46.
- Lau ASN, Mruk DD. Rab8B GTPase and junction dynamics in the testis. *Endocrinology*. 2003;144:1549–1563.
- Lee NPY, Mruk DD, Conway AM, Cheng CY. Zyxin, axin, and Wiskott-Aldrich syndrome protein are adaptors that link the cadherin/catenin protein complex to the cytoskeleton at adherens junctions in the seminiferous epithelium of the rat testis. *J Androl*. 2004;25:200–215.
- Lee NPY, Mruk D, Lee WM, Cheng CY. Is the cadherin/catenin complex a functional unit of cell-cell-actin-based adherens junctions (AJ) in the rat testis? *Biol Reprod*. 2003;68:489–508.
- Lock JG, Stow JL. Rab11 in recycling endosomes regulates the sorting and basolateral transport of E-cadherin. *Mol Biol Cell*. 2005;16:1744–1755.
- Marzesco AM, Dunia I, Pandjaitan R, Recouvreur M, Dauzonne D, Benedetti EL, Louvard D, Zahraoui A. The small GTPase Rab13 regulates assembly of functional tight junctions in epithelial cells. *Mol Biol Cell*. 2002;13:1819–1831.
- Maxfield FR, McGraw TE. Endocytic recycling. *Nat Rev Mol Cell Biol*. 2004;5:121–132.
- Mays RW, Beck KA, Nelson WJ. Organization and function of the cytoskeleton in polarized epithelial cells: a component of the protein sorting machinery. *Curr Opin Cell Biol*. 1994;6:16–24.
- Moroi S, Saitou M, Fujimoto K, Sakakibara A, Furuse M, Yoshida O, Tsukita S. Occludin is concentrated at tight junctions of mouse/rat but not human/guinea pig Sertoli cell testes. *Am J Physiol*. 1998;274:C1708–C1717.
- Mruk D, Cheng CH, Cheng YH, Mo MY, Grima J, Silvestrini B, Lee WM, Cheng CY. Rat testicular extracellular superoxide dismutase (SOD<sub>EX</sub>): its purification, cellular distribution, and regulation. *Biol Reprod*. 1998;59:298–308.
- Mruk D, Cheng CY. Sertolin is a novel gene marker of cell-cell interactions in the rat testis. *J Biol Chem*. 1999;274:27056–27068.
- Mruk DD, Cheng CY. Sertoli-Sertoli and Sertoli-germ cell interactions and their significance in germ cell movement in the seminiferous epithelium during spermatogenesis. *Endocr Rev*. 2004;25:747–806.
- Mruk DD, Siu MKY, Conway AM, Lee NPY, Lau ASN, Cheng CY. Role of tissue inhibitor of metalloproteases-1 in junction dynamics in the testis. *J Androl*. 2003;24:510–523.

- Nagelkerken B, Van Anken E, Van Raak M, Gerez L, Mohrmann K, Van Uden N, Holthuizen J, Pelkmans L, Van der Sluijs P. Rabaptin4, a novel effector of the small GTPase Rab4A, is recruited to perinuclear recycling vesicles. *Biochem J.* 2000;346:593–601.
- Page M, Thorpe R. Purification of IgG by precipitation with sodium sulfate or ammonium sulfate. In: Walker JM, ed. *The Protein Protocols Handbook*. Totowa, NJ: Humana Press; 2001a:983–984.
- Page M, Thorpe R. Purification of IgG using DEAE-Sepharose chromatography. In: Walker JM, ed. *The Protein Protocols Handbook*. Totowa, NJ: Humana Press; 2001b:987–988.
- Palacios F, Price L, Schweitzer J, Collard JG, D'Souza-Schorey C. An essential role for ARF6-regulated membrane traffic in adherens junction turnover and epithelial cell migration. *EMBO J.* 2001;20:4973–4986.
- Palacios F, Tushir JS, Fujita Y, D'Souza-Schorey C. Lysosomal targeting of E-cadherin: a unique mechanism for the down-regulation of cell-cell adhesion during epithelial to mesenchymal transitions. *Mol Cell Biol.* 2005;25:389–402.
- Palombi F, Di Carlo C. Alkaline phosphatase is a marker for myoid cells in cultures of rat peritubular and tubular tissue. *Biol Reprod.* 1988;39:1101–1109.
- Parvinen M, Ruokonen A. Endogenous steroids in the rat seminiferous tubules. Comparison of the stages of the epithelial cycle isolated by transillumination-assisted microdissection. *J Androl.* 1982;3:211–220.
- Parvinen M, Vanha-Perttula T. Identification and enzyme quantification of the stages of the seminiferous epithelial wave in the rat. *Anat Rec.* 1972;174:435–450.
- Perez-Moreno M, Jamora C, Fuchs E. Sticky business: orchestrating cellular signals at adherens junctions. *Cell.* 2003;112:535–548.
- Pol A, Ortega D, Enrich C. Identification of cytoskeleton-associated proteins in isolated rat liver endosomes. *Biochem J.* 1997;327:741–746.
- Qualmann B, Kessels NM, Kelly RB. Molecular links between endocytosis and the actin cytoskeleton. *J Cell Biol.* 2000;150:F111–F116.
- Russell LD. Form, dimensions, and cytology of mammalian Sertoli cells. In: Russell LD, Griswold MD, eds. *The Sertoli Cell*. Clearwater, Fla: Cache River Press; 1993:1–37.
- Russell LD, Bartke A, Goh JC. Postnatal development of the Sertoli cell barrier, tubular lumen, and cytoskeleton of Sertoli and myoid cells in the rat, and their relationship to tubular fluid secretion and flow. *Am J Anat.* 1989;184:179–189.
- Seabra MC, Coudrier E. Rab GTPases and myosin motors in organelle motility. *Traffic.* 2004;5:393–399.
- Seachrist JL, Ferguson SSG. Regulation of G-protein coupled receptor endocytosis and trafficking by Rab GTPases. *Life Sci.* 2003;74:225–235.
- Sheth B, Fontaine JJ, Ponza E, McCallum A, Page A, Citi S, Louvard D, Zahraoui A, Fleming TP. Differentiation of the epithelial apical junctional complex during mouse preimplantation development: a role for Rab13 in the early maturation of the tight junction. *Mech Dev.* 2000;97:93–104.
- Silvestrini B, Palazzo G, De Gregorio M. Lonidamine and related compounds. *Prog Med Chem.* 1984;21:110–135.
- Somsel Rodman J, Wandinger-Ness A. Rab GTPases coordinate endocytosis. *J Cell Sci.* 2000;113:183–192.
- Stenmark H, Olkkonen VM. The Rab GTPase family. *Genome Biol.* 2001;2:3007.3001–3007.3007.
- Takai Y, Sasaki T, Matozaki T. Small GTP-binding proteins. *Physiol Rev.* 2001;81:153–208.
- Vitale G, Rybin V, Christoforidis S, Thornqvist PO, McCaffrey M, Stenmark H, Zerial M. Distinct Rab-binding domains mediate the interaction of rabaptin-5 with GTP-bound Rab4 and Rab5. *EMBO J.* 1998;17:1941–1951.
- Vitale R, Fawcett DW, Dym M. The normal development of the blood-testis barrier and the effects of clomiphene and estrogen treatment. *Anat Rec.* 1973;176:333–344.
- Wright WW, Zabudoff SD, Penttila TL, Parvinen M. Germ cell-Sertoli cell interactions: regulation by germ cells of the stage-specific expression of CP-2/cathepsin L mRNA by Sertoli cells. *Dev Genet.* 1995;16:104–113.
- Xia W, Cheng CY. TGF- $\beta$ 3 regulates anchoring junction dynamics in the seminiferous epithelium of the rat testis via the Ras/ERK signaling pathway: an in vivo study. *Dev Biol.* 2005;280:321–343.
- Yeaman C, Grindstaf KK, Nelson WJ. New perspectives on mechanisms involved in generating epithelial cell polarity. *Physiol Rev.* 1999;79:73–98.
- Zahraoui A, Touchot N, Chardin P, Tavitian A. Complete coding sequences of the Ras related Rab 3 and 4 cDNAs. *Nucleic Acids Res.* 1988;16:1204.
- Zerial M, McBride H. Rab proteins as membrane organizers. *Nat Rev Mol Cell Biol.* 2001;2:107–117.
- Zwain IH, Cheng CY. Rat seminiferous tubular culture medium contains a biological factor that inhibits Leydig cell steroidogenesis: its purification and mechanism of action. *Mol Cell Endocrinol.* 1994;104:213–227.